

Broad [OIII] in the globular cluster RZ 2109: X-ray ionized nova ejecta?

E. Ripamonti^{1,2}, M. Mapelli²

¹*Università di Milano-Bicocca, Dipartimento di Fisica G. Occhialini, Piazza delle Scienze 3, I-20126, Milano, Italy*

²*INAF - Osservatorio Astronomico di Padova, Vicolo dell'Osservatorio 5, I-35122, Padova, Italy*

21 November 2018

ABSTRACT

We study the possibility that the very broad ($\sim 1500 \text{ km s}^{-1}$) and luminous ($L_{5007} \sim 1.4 \times 10^{37} \text{ erg s}^{-1}$) [OIII] line emission observed in the globular cluster RZ 2109 might be explained with the photoionization of nova ejecta by the bright ($L_X \sim 4 \times 10^{39} \text{ erg s}^{-1}$) X-ray source hosted in the same globular cluster. We find that such scenario is plausible and explains most of the features of the RZ 2109 spectrum (line luminosity, absence of H emission lines, peculiar asymmetry of the line profile); on the other hand, it requires the nova ejecta to be relatively massive ($\gtrsim 0.5 \times 10^{-3} M_\odot$), and the nova to be located at a distance $\lesssim 0.1 \text{ pc}$ from the X-ray source. We also predict the time evolution of the RZ 2109 line emission, so that future observations can be used to test this scenario.

Key words: novae, cataclysmic variables - galaxies: individual (NGC 4472) - galaxies: star clusters: individual (RZ 2109) - X-rays: binaries - ISM: jets and outflows

1 INTRODUCTION

Many X-ray sources (XRSs) are inside globular clusters (GCs; e.g. Heinke 2011), but only five of them unambiguously host a black hole (BH; Maccarone et al. 2007, hereafter M07; Brassington et al. 2010; Shih et al. 2010; Maccarone et al. 2011; Irwin et al. 2010, hereafter I10; see King 2011 for an alternative explanation). These five objects were observed as luminous XRSs ($L_X \gtrsim 4 \times 10^{38} \text{ erg s}^{-1}$) with strong variability (so that blending is excluded; Kalogera et al. 2004).

The spectra of at least two of their host GCs are quite peculiar. One of them, RZ 2109 (in the elliptical NGC 4472; Zepf et al. 2007, 2008, and Steele et al. 2011; hereafter Z07, Z08, S11) displays prominent and broad [OIII] $\lambda\lambda 5007, 4959$ emission (the FWHM of [OIII] $\lambda 5007$ is $1000\text{--}2000 \text{ km s}^{-1}$; its flux is $F_{5007} \sim 4.4 \times 10^{-16} \text{ erg s}^{-1} \text{ cm}^{-2}$; at $D = 16 \text{ Mpc}$ it corresponds to $L_{5007} \sim 1.4 \times 10^{37} \text{ erg s}^{-1}$; see Z08), but no H line emission¹. The spectrum of the GC hosting the XRS CXOJ033831.8-352604 (in the elliptical NGC 1399; see I10) is somewhat similar in the absence of H and the presence of [OIII] lines; but widths and luminosities are lower (FWHM $\simeq 140 \text{ km s}^{-1}$, $L_{5007} \sim \text{few} \times 10^{36} \text{ erg s}^{-1}$), and [NII] $\lambda\lambda 6583, 6548$ emission is comparable to [OIII].

These observations are hard to explain, because of the high [OIII]/H β ratio (Z08 estimate ~ 30 ; I10 finds a 3σ lower limit of 5; both are very uncertain) and of the large broadening, implying motions much faster than GC velocity

($\sim 10 \text{ km s}^{-1}$). Optical lines are too wide for a planetary nebula, and too narrow for a supernova remnant. Z08 suggest that the [OIII] emission from RZ 2109 might come from a strong wind originating around the BH, photoionized by the XRS. Such scenario strongly favours a BH with mass $\approx 10 M_\odot$, rather than an intermediate-mass BH (IMBH) with mass in the $10^2\text{--}10^5 M_\odot$ range. This was preferred to the hypothesis that the [OIII]-emitting gas closely orbits ($r \sim 10^{13} \text{ cm}$) an IMBH, on the basis of considerations about the maximum possible emission from such a small volume. Such argument is severely weakened if the orbiting gas is very metal-rich, e.g. as the result of the tidal disruption of a white dwarf (WD) by an IMBH (see I10): according to Porter (2010), the CXOJ033831.8-352604 data are compatible with this scenario, whereas in the case of RZ 2109 the conflict remains; however, Clausen & Eracleous (2011) showed that simulations of WD disruption can reproduce the [OIII] line profiles observed in RZ 2109. On the other hand, Maccarone & Warner (2011) argued that the line emission of CXOJ033831.8-352604 might be better explained with the photoionization (by the XRS) of the wind from an R Corinae Borealis star in the same GC.

In this paper, we examine a further possible scenario, and apply it to the case of RZ 2109: [OIII] lines might be associated with a recent nova eruption in the core of the GC. In particular, we discuss the case (first mentioned by S11) where the [OIII] emission comes from the photoionization of the nova ejecta by the XRS. X-ray emission from novae is typically fainter ($L_X \sim 10^{38} \text{ erg s}^{-1}$, even though at least one nova was reported to reach $L_X \gtrsim 10^{39} \text{ erg s}^{-1}$ - see

¹ No other emission line (e.g. [OII] $\lambda 3727$, [NII] $\lambda\lambda 6548, 6583$, [SII] $\lambda\lambda 6716, 6731$) is detected, except perhaps [OIII] $\lambda 4363$.

Henze et al. 2010) and shorter (decay times $\lesssim 1$ yr) than what is observed for these sources. Thus, we assume that the nova eruption is *not* associated to the XRS, i.e. that the co-existence of the two phenomena in the same GC is serendipitous.

2 NOVAE

Nova eruptions occur in binary systems where a WD accretes from a normal star (e.g. Gehrz et al. 1998). Nuclear reactions ignite explosively in the material accumulated on the WD surface, leading to a brief super-Eddington phase during which the WD outer layers are ejected (e.g. Starfield et al. 1972, Prialnik 1986). Ejecta velocities are in the 100–2500 km s⁻¹ range, and their metal mass fractions can be as high as $Z \sim 0.5$ (Yaron et al. 2005, Shara et al. 2010; hereafter Y05, S10). Typical ejecta masses are in the 10^{-5} – $10^{-4} M_{\odot}$ range; but Y05 and S10 showed that nova eruptions on slowly-accreting, low-temperature WDs can eject up to $\sim 2.2 \times 10^{-3} M_{\odot}$ of gas. Ejecta mass estimates in X-ray detected novae (Pietsch et al. 2007) somewhat confirm theoretical expectations: ejecta masses of $\geq 10^{-3} M_{\odot}$ are likely in at least 2 out of 18 novae.

WD-hosting binaries are common in GCs (Sigurdsson & Phinney 1995); thus, novae should be frequent in GCs. This disagrees with the low number of novae observed in GCs²; but the discrepancy might be explained by observational biases. We parametrize the nova rate in a GC as $\Gamma_{GC} = \gamma_{GC} \Gamma_E M_{GC}$, where $\Gamma_E \sim 2.2 \times 10^{-10} \text{ yr}^{-1} M_{\odot}^{-1}$ is the nova rate per unit stellar mass in elliptical galaxies (Della Valle et al. 1994; Mannucci et al. 2005; Henze et al. 2009), M_{GC} is the GC mass, and γ_{GC} is the enhancement of the nova rate in GCs (compared to ellipticals). We expect $\gamma_{GC} \gtrsim 1$ because of the over-abundance of WD-hosting binaries in GCs. On the other hand, observations of the M31 and M87 GC systems can put upper limits on nova occurrence rates: for M87, Shara et al. (2004) infer $\Gamma_{GC, M87} \sim 0.004 \text{ yr}^{-1} \text{ GC}^{-1}$, whereas for M31 we have an upper limit $\Gamma_{GC, M31} \lesssim 0.005 \text{ yr}^{-1} \text{ GC}^{-1}$ (Henze et al. 2009); assuming $M_{GC} \sim 10^6 M_{\odot}$, these rates imply $\gamma_{GC} \lesssim 20$.

3 MODELLING OF LINE EMISSION

We use the photoionization code `CLOUDY` (version 08.00, see Ferland et al. 1998) to model the optical spectrum resulting from the photoionization of the nova ejecta by the XRS.

We represent the nova ejecta as a slab of material with thickness Δd , number density n , filling factor f_{fill} , and metallicity Z , at a distance d from the XRS, covering a fraction f_{cov} of the solid angle around it. We note that f_{cov} determines two different geometrical configurations:

(i) if f_{cov} is large (≥ 0.5), the XRS must be *within* the nova ejecta. In such case, we neglect the offset between the XRS and the centre of the ejecta shell, so that the radius

² We are aware of 5 GC novae: 2 in Milky Way GCs, 2 in M31, 1 in M87; see Shara et al. (2004), Shafter & Quimby (2007), Henze et al. (2009), Moore & Bildsten (2011); a sixth nova candidate (in a M31 GC) was reported by Peacock et al. (2010).

Table 1. Explored parameter space.

Parameter	Range of values
$\log d$ [cm]	16–18.5, with 0.25 steps
$\log \Delta d$ [cm]	15.0, 15.5, 16, 16.5
f_{cov}	0.003, 0.01, 0.03, 0.1, 2/3
$\log n$ [cm ⁻³]	-2 to 10, with 0.1 steps
f_{fill}	2/3
Z	0.14, 0.29, 0.50
kT [keV]	0.22
$L_{0.2-10}^{(a)}$ [erg s ⁻¹]	4.5×10^{39}
$\log N_{\text{H}}$ [cm ⁻²]	19, 20, 21, 21.5
m_{ej} [M_{\odot}]	$\leq 10^{-2}$

Definitions: d is the distance from the XRS to the WD that produced the nova eruption; Δd is the thickness of the nova shell; f_{cov} is the covering factor of the nova shell (as seen from the XRS); n is the number density of the nova shell ($n \equiv \rho/m_{\text{H}}$, where m_{H} is the mass of the H atom); f_{fill} is the filling factor of the nova shell; Z is the mass fraction of metals; kT is the temperature of the blackbody spectrum of the XRS; $L_{0.2-10}$ is the luminosity of the XRS in the band 0.2–10 keV; N_{H} is the column density that the radiation from the XRS must cross before reaching the nova shell; m_{ej} is the mass of the ejecta shell.

Notes: ^(a): derived assuming a distance $D = 16$ Mpc.

of the ejecta shell is $r_{\text{ej}} \sim d$; then, the time elapsed after the nova explosion is $t_{\text{nova}} \sim r_{\text{ej}}/v_{\text{ej}} \simeq 30 \text{ yr } d_{17} v_{\text{ej},3}^{-1}$, where $d_{17} \equiv d/(10^{17} \text{ cm})$, and $v_{\text{ej},3} \equiv v_{\text{ej}}/(10^3 \text{ km s}^{-1})$.

(ii) if f_{cov} is small, we assume the XRS to be *outside* the ejecta, and estimate r_{ej} from simple geometry: $f_{\text{cov}} \simeq (\pi r_{\text{ej}}^2)/(4\pi d^2)$, so that $t_{\text{nova}} \sim 2\sqrt{f_{\text{cov}}}(d/v_{\text{ej}}) \simeq 6 \text{ yr } (f_{\text{cov}}/0.01)^{1/2} d_{17} v_{\text{ej},3}^{-1}$.

The XRS spectrum was taken from M07: we use a disk blackbody spectrum with $kT = 0.22$ keV and 0.2–10 keV luminosity $\sim 4.5 \times 10^{39} \text{ erg s}^{-1}$. We note that M07 reported a large variation (a drop by a factor of ~ 7) in the count rate during a single *XMM-Newton* observation. Such variation is consistent with an increase in the intervening column density, from $N_{\text{H}} \simeq 1.67 \times 10^{20} \text{ cm}^{-2}$ (consistent with the Galactic value) to $N_{\text{H}} \sim 3 \times 10^{21} \text{ cm}^{-2}$. Thus, we assume that the intrinsic X-ray spectrum does not change; but we experiment with different N_{H} values.

Table 1 describes the extent of the explored parameter space. We point out that:

(i) We use the `CLOUDY` pre-defined nova abundance set. It represents typical nova ejecta³, and corresponds to an O/H number ratio of 1.7×10^{-2} (~ 30 times larger than in the solar mixture), and to a metal mass fraction $Z \simeq 0.29$. We obtain mixtures with different metallicities by rescaling the metal abundances of this set by a factor 0.4 ($Z = 0.14$) or 2.5 ($Z = 0.50$).

(ii) The slab mass is $m_{\text{ej}} = 4\pi d^2 \Delta d f_{\text{cov}} f_{\text{fill}} n m_{\text{H}} \simeq 10^{-2} M_{\odot} d_{17}^2 [\Delta d/(10^{16} \text{ cm})] f_{\text{cov}} f_{\text{fill}} [n/(10^4 \text{ cm}^{-3})]$, where

³ From Ferland & Shields 1978, based on observations of nova V1500 Cygni; solar abundances (from Grevesse & Sauval 1998, Holweger 2001, Allende Prieto, Lambert & Asplund 2001, 2002) were used for elements not listed in that paper.

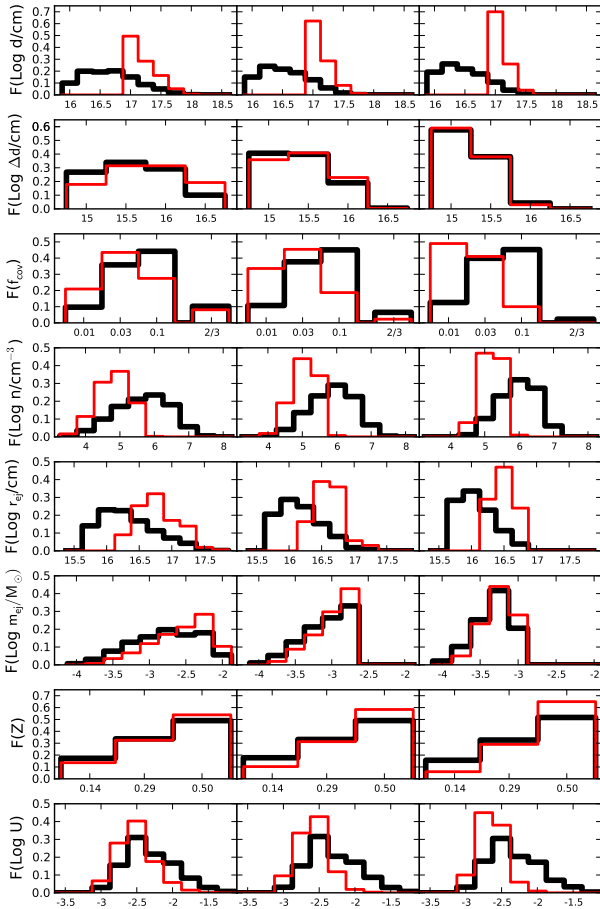


Figure 1. Distribution of parameters for the viable models. Each row shows the distribution of one parameter (see the caption of Table 1; in addition, U is the ionization parameter); columns correspond to different priors on the ejecta mass m_{ej} (left: $\leq 10^{-2} M_{\odot}$; centre: $\leq 2.5 \times 10^{-3} M_{\odot}$; right: $\leq 10^{-3} M_{\odot}$). The thick lines refer to all the viable models within the m_{ej} limit, whereas the thin (red on the web) lines further require the distance d of the nova from the XRS to be $\geq 10^{17}$ cm. The distributions are normalized to the number of viable models satisfying the relevant prior (so, the thin line is often above the thick line even if it refers to a lower number of viable models).

$m_{\text{H}} = 1.67 \times 10^{-24}$ g is the mass of the H atom. Since we expect that $m_{\text{ej}} \lesssim 2.2 \times 10^{-3} M_{\odot}$ (Y05, S10), ionization models were calculated only when $m_{\text{ej}} \leq 0.01 M_{\odot}$.

4 COMPARISON OF MODELS AND DATA FOR RZ 2109

Models were required to agree with two basic observational constraints from the spectrum shown in Z08⁴

⁴ The Z08 spectrum (taken in December 2007) is quite similar to the other three spectra of RZ 2109 discussed in S11 (and taken in the following ~ 1.3 years). Instead the two spectra described by Z07 (taken in 2004–2005, i.e. in the previous ~ 3.9 years) appear quite different (FWHM ~ 200 – 350 km s⁻¹, $F_{5007} \sim 0.13 \times 10^{-16}$ erg s⁻¹ cm⁻²). Z07 warn that uncertain-

(i) the flux of the [OIII] λ 5007 line, $F_{5007} \simeq 4.4 \times 10^{-16}$. Z08 do not quote an error on this measurement: the equivalent width comparison performed by S11 suggests an uncertainty of 20–30 per cent; but the discrepancy with the Z07 spectrum suggests a larger amount. Furthermore, we account for the approximations of the ionization models by increasing such uncertainty. Thus, we consider viable models with F_{5007} within a factor of 3 from the Z08 estimate.

(ii) The absence of any other emission lines in all the spectra: we exclude all the models where the luminosity in any optical line⁵ exceeds $0.1L_{5007}$.

About 4 per cent of the models we calculated⁶ satisfy the above criteria. In Fig. 1, we show the distribution of the various parameters (including the ionization parameter, defined as the number ratio of ionizing photons to H atoms, $U = Q(H)/(4\pi d^2 cn)$, where $Q(H)$ is the number of ionizing photons - i.e. with energy ≥ 13.6 eV - emitted by the XRS in the unit time) for these viable models, and how these distributions are influenced by the choice of priors about the models (e.g. the effects of using different thresholds on the ejecta mass, or imposing a minimum for the nova-XRS distance). Such distributions show us where a large amount of parameter space is available. It can be seen that:

(i) it is almost impossible to have viable models if $d \gtrsim 10^{17.5}$ cm $\simeq 0.1$ pc;

(ii) thin shells ($\Delta d \lesssim 10^{16}$ cm) are favoured, especially when high- m_{ej} models are excluded;

(iii) models where the XRS is inside the nova shell (i.e. with $f_{\text{cov}} \geq 0.5$) are moderately unlikely, especially when high- m_{ej} models are excluded;

(iv) shell densities are in the $10^4 \lesssim n/\text{cm}^{-3} \lesssim 10^7$ range; but models with high values of d show a narrower distribution, favouring the low- n part;

(v) $Z = 0.5$ models are favoured; but it is possible to get reasonable results if $Z = 0.29$ or even $Z = 0.14$.

(vi) The ionization parameter is mostly close to $\log(U) \sim -2.5$, a fairly typical value for HII regions; this is somewhat remarkable, as the ionizing spectrum is not produced by hot stars, and most of the radiation energy is in the form of quite energetic (0.1–1 keV) photons (rather than photons just above the Lyman limit).

5 DISCUSSION

5.1 Predictions

[OIII] emission should evolve on a timescale t_{nova} . Thus, our scenario can be tested by monitoring the RZ 2109 spectrum.

We arbitrarily select four viable models (see Table 2) for a study of the time evolution of line emission. This was

ties amount to a factor of $\gtrsim 2$, and the discrepancy might be explained by the (very different) observational setups.

⁵ We actually considered only H α , H β , [OI] λ 6300, [OII] λ 3727, [NII] λ 6548, 6583, and [SII] λ 6716, 6731.

⁶ We calculated a total of ~ 53000 models, of whom 2144 are viable (655 if we consider only models with $d \geq 10^{17}$ cm). If we require $m_{\text{ej}} \leq 2.5 \times 10^{-3} M_{\odot}$ the number of viable models is 1278 (262 if we further impose $d \geq 10^{17}$ cm), and requiring $m_{\text{ej}} \leq 10^{-3} M_{\odot}$ further decreases this number to 652 (100 of whom have $d \geq 10^{17}$ cm).

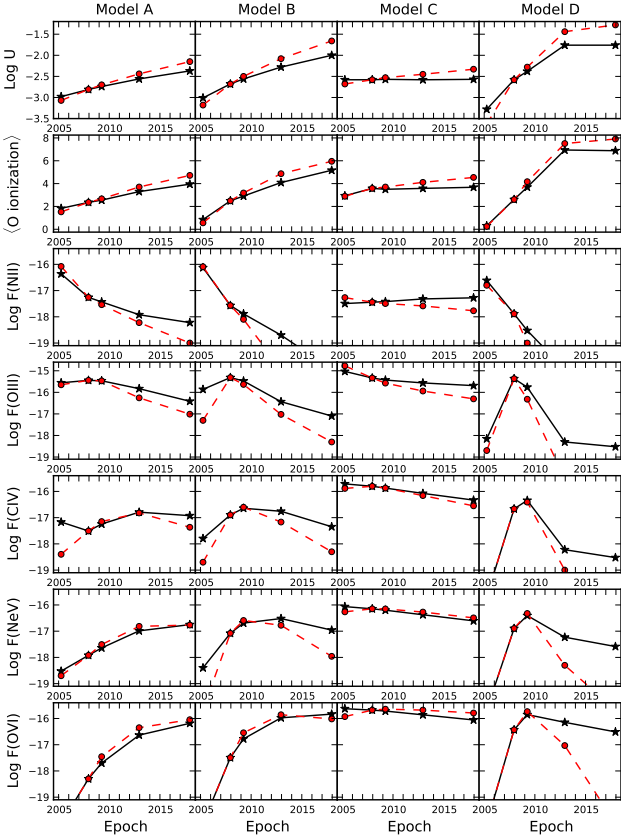


Figure 2. Temporal evolution of model predictions for the four representative models described in the text; solid lines with star symbols are based on assumption (a) (i.e. that the shell thickness is constant), and dashed lines with round symbols (red on the web) are based on assumption (b) (i.e. that shell thickness is proportional to the ejecta radius). Each column refers to one of those models (model A to model D, from left to right), and all the plots have time on the x-axis. On the y-axis we show the ionization parameter U (this is actually an assumption of the model, rather than a prediction; first row from the top), the average ionization stage of oxygen (i.e. $\sum_i (if_{O,i})$, where $f_{O,i}$ is the fraction of O atoms that is ionized i times; second row), and the flux at Earth (in $\text{erg s}^{-1} \text{cm}^{-2}$) of five different lines or groups of lines ([NII] $\lambda\lambda 6548, 6583\text{\AA}$, third row; [OIII] $\lambda 5007\text{\AA}$, fourth row; CIV $\lambda\lambda 1549, 1551\text{\AA}$, fifth row; [NeV] $\lambda 3426\text{\AA}$, sixth row; the complex of OVI lines between $\lambda 1032\text{\AA}$ and $\lambda 1038\text{\AA}$, seventh row).

done by assuming that the nova shell keeps expanding with $v_{\text{ej},3} \simeq 1.5$ (cfr. Z08, S11), and properly scaling the relevant parameters (f_{cov} , Δd and n if XRS is outside the expanding shell; d , Δd and n otherwise). As the evolution of the thickness Δd of the nova shell is unclear, we consider two different cases: (a) $\Delta d = \text{constant}$ (appropriate for small velocity dispersions within the ejecta), and (b) $\Delta d \propto r_{\text{ej}}$ (appropriate for a significant ejecta velocity dispersion).

We calculated the properties of each of these four models at five times: three past epochs (April 2005, December 2007, and March 2009, i.e. the times of the last Z07 observation, of the Z08 observation, and of the last S11 observation, respectively), and two future ones (December 2012 and December 2017, i.e. 5 and 10 years after the Z08 observation). The behaviour of the results are summarized in Fig. 2, where we show the time evolution of the ionization parameter, of

Table 2. Parameters of selected models.

Parameter	Model A	Model B	Model C	Model D
$\log d$ [cm]	17.25	17.00	16.75	16.50
$\log \Delta d$ [cm]	15.5	15.0	15.0	15.5
f_{cov}	0.03	0.03	2/3	0.10
$\log n$ [cm^{-3}]	4.7	5.5	5.0	5.5
$\log U(13.6\text{eV})$	-2.81	-2.68	-2.58	-2.58
Z	0.50	0.29	0.50	0.29
$\log n_{\text{H}}$ [cm^{-2}]	21	20	21.5	21.5
m_{ej} [$10^{-4} M_{\odot}$]	10.6	6.7	14.9	7.0
r_{ej} [10^{16} cm]	6.2	3.5	5.6	2.0
t_{nova} [yr]	13.1	7.4	11.9	4.2

Parameters not included in this list (e.g. $L_{0.2-10}$) are fixed at the values in Table 1; the values given here refer to the epoch of the Z08 spectrum (December 2007). The estimate of t_{nova} assumes $v_{\text{ej},3} = 1.5$.

the ionization state of Oxygen, and of the intensities of five lines (or groups of lines). Such lines are representative of the main ionization stages and of the most abundant heavy elements in the ejecta, but are *not* always the most intense: an exhaustive list of possibly detectable optical and UV lines can be found in the Appendix.

In 7 out of 8 models the ionization parameter increases with time, so that heavy elements (such as oxygen) move to higher ionization states. Therefore, high-ionization lines (such as the OVI lines around $\lambda 1035\text{\AA}$) tend to grow stronger, whereas low-ionization lines (e.g. [NII] $\lambda\lambda 6548, 6583\text{\AA}$) tend to weaken with time, and intermediate-ionization lines (e.g. the CIV doublet at $\lambda\lambda 1549, 1551\text{\AA}$) grow to a peak, and then start to decline.

The case (a) of model C is the main exception: since it assumes that (i) the XRS is within the expanding shell, and (ii) the shell thickness is constant, the density evolution in the shell ($n \propto r_{\text{ej}}^{-2}$) compensates the geometrical dilution of the ionizing flux, resulting in a constant ionization parameter. As a consequence, the ionization state of Oxygen (and of all the other heavy elements) remains practically constant, and line fluxes tend to decrease very slowly.

The four models were required to agree with the December 2007 observations, so their spectra for this epoch are dominated by the [OIII] doublet, with F_{5007} within 20 per cent from the Z08 value. In addition, [NeIII] $\lambda 3869$ and [OIII] $\lambda 4363$ might be strong enough to be detectable: the latter was marginally detected by Z08; as to [NeIII], we note that the Z08 spectrum is very noisy at $\lambda \lesssim 4000\text{\AA}$, and this line might be confused with other features in that region. All the models (except model D - see next subsection) are in quite satisfactory agreement with the 2009 observation, too: this is simply because the 1.3 years interval from December 2007 to March 2009 is a relatively small fraction of t_{nova} .

Instead we find larger (and more interesting) differences if we look at the April 2005 spectrum: models A and C predict that the [OIII] emission was as strong (A) or stronger (C) than in 2007, and require that the discrepancy among the fluxes reported by Z07 and Z08 derives from observational factors only. Instead, models B and D provide a dif-

ferent explanation: their quite short t_{nova} imply large differences in r_{ej} : in 2005 r_{ej} was only 2/3 (model B) or 1/3 (model D) of its value in 2007; such a difference not only reduces the amount of energy intercepted by the ejecta, but at the same time lowers the ionization parameter, favouring low-ionization states and moving the emission from [OIII] to [OII] (or even [OI]) lines.

The predictions for 2012 and 2017 offer an opportunity to test these models, with model D predicting that all anomalous emission lines should disappear before 2012, model B predicting large declines, and models A and C predicting a slower, steady decline. As we already mentioned, such decline is mostly understood in terms of an increasing ionization parameter, so that the O^{++} abundance drops.

5.1.1 Modelling issues

It should be noted that all the above predictions suffer from a number of approximations:

(i) The structure of a nova shell is not uniform. There are large density fluctuations both at early times ($\lesssim 2$ years after the eruption; see e.g. the images of Nova Cygni 1992 in Chochol et al. 1997) and at late times ($\gtrsim 10$ years after the eruption; see e.g. the images of T Pyx in Shara et al. 1997).

(ii) The residual nuclear burning on the WD responsible for the nova eruption might produce a significant amount of UV/X-ray photons for a few years (see Henze et al. 2010): furthermore, when $t_{\text{nova}} \lesssim 2\text{yr}$, $r_{\text{ej}} \leq 10^{16}\text{cm} \ll d$, and even moderate WD luminosities (say $L_{\text{X,WD}} \sim 10^{38}\text{erg s}^{-1}\text{cm}^{-2}$) are enough for the WD emission to dominate over the one from the XRS. Therefore, the predictions for model B in 2005, for model D in 2007, and especially for model D in 2005 might suffer from the fact that our models do not consider the WD emission.

(iii) The *CLOUDY* calculations assume steady state, but models with a long ($\gtrsim 1$ yr) recombination timescale would require a time-dependent approach. For H recombination, $t_{\text{rec,H}} \sim (\alpha_{\text{A}} n)^{-1} \simeq 0.8 (n/10^5\text{cm}^{-3})^{-1}\text{yr}$ (where $\alpha_{\text{A}} \sim 4 \times 10^{-13}\text{cm}^3\text{s}^{-1}$ is the H recombination coefficient), so that models with $n \lesssim 10^5\text{cm}^{-3}$ might suffer from this problem; however, the recombination timescales of highly ionized metals are shorter (by factors of 2–10) than $t_{\text{rec,H}}$, and predictions about their lines should be reliable for $n \gtrsim 10^4\text{cm}^{-3}$.

(iv) Our geometry is extremely simple, and might suffer from assuming that the whole nova shell is at the same distance from the XRS: this is reasonable if the XRS is within the shell (model C), or if $r_{\text{ej}} \ll d$, but there are a number of cases (models A and B at the 2012 and 2017 epochs; model D at all epochs except 2005) where $r_{\text{ej}} \geq d/2$ (so that the ionization parameter in the XRS-approaching part of the shell might be ≥ 9 times higher than in the XRS-receding part)⁷.

(v) The timing of the evolution depends upon the exact value of $v_{\text{ej},3}$: the adopted 1.5 value is reasonable (S11 estimates $v_{\text{ej},3} \simeq 1.3$ for the broad component of the line profile

- see the next subsection), but not unique: a lower(higher) choice of v_{ej} would delay(fasten) the predicted evolution (for example, if $v_{\text{ej}} = 1$, our predictions for December 2012 and December 2017 would apply to June 2015 and December 2022, respectively). This is particularly relevant for Model D: the [OIII] flux in Fig. 2 and Table A4 evolves too rapidly (the 2007 flux agrees with the observations, but both the 2005 and the 2009 fluxes are too low); however, the model should not be discarded (yet) because these discrepancies can still be reconciled using a value of $v_{\text{ej},3} (\simeq 1)$ that is still in agreement with the S11 measurements.

Some of these issues might be resolved by adopting more complicated modelling (e.g. assume a spectrum/temporal evolution for the WD emission, use some density distribution, adopt a more realistic geometry, etc.); however, a more detailed modelling, while providing more reliable predictions, would also require us to introduce a number of additional parameters. This is not only a problem in terms of resources (such as computing power), but would further complicate the interpretation of the results.

5.2 Line profile

S11 model the spectral profile of the [OIII] $\lambda\lambda 4959, 5007$ complex as the superposition of the identical profiles of the two lines of the doublet, each one made of a central, relatively narrow ($\text{FWHM} \sim 300\text{km s}^{-1}$) gaussian peak, plus a much broader ($\text{FWHM} \sim 1300\text{km s}^{-1}$) ‘flat’ component (possibly the result of a bipolar outflow); notably, the latter component is not really flat: the red side is about 1.4 times brighter than the blue side. As noted by S11, this is consistent with a nova shell between the XRS and the observer⁸. If this is the case, the flux difference among the two sides suggests that in 2007–2008 r_{ej} was of the order of 10 per cent of the distance between the nova and the XRS: this would favor models with $f_{\text{cov}} \sim 0.01$. Furthermore, since r_{ej} increases with time, the asymmetry between the red and blue sides should increase as well (at least as long as the XRS is outside the nova shell).

If the nova lies between us and the XRS, the ejecta might even intercept the line of sight to the XRS, increasing the value of N_{H} . We checked whether such an increase can explain the fading of the XRS seen in the 2004 *XMM* observation (see M2007), and in the subsequent *Swift* and *Chandra* observations (see Maccarone et al. 2010). The effective X-ray extinction due to isotropic nova ejecta is

$$N_{\text{H,shell}} = g \frac{m_{\text{ej}}}{4\pi r_{\text{ej}}^2 m_{\text{H}}} \frac{Z}{Z_{\odot}} \simeq \simeq 4.2 \times 10^{22}\text{cm}^{-2} \left(\frac{g}{3}\right) \left(\frac{m_{\text{ej}}}{10^{-3}\text{M}_{\odot}}\right) \left(\frac{r_{\text{ej}}}{10^{16}\text{cm}}\right)^{-2} \left(\frac{Z}{0.29}\right) (1)$$

where g is a geometrical factor accounting for the number

⁸ S11 also note that a nova shell fails to explain why the line profile is made of 2 components. We do not attempt to build a model, but it is quite likely that such a profile can be reproduced if the shell density is not uniform. Alternatively, the nova shell might be made of a slow ($v \sim 300\text{km s}^{-1}$) isotropic component, plus a fast bipolar one ($v \sim 1300\text{km s}^{-1}$). Nova observations (e.g. Iijima & Naito 2011) and theoretical models (see e.g. the ejecta velocity plots in S10) support these hypotheses by finding/predicting complex profiles for nova emission lines.

⁷ Epochs 2012 and 2017 of model D are extreme cases, since we have $r_{\text{ej}} > d$, and the XRS is engulfed by the shell; we try to adapt to the new situation by switching to a model with the XRS at the centre of the shell ($f_{\text{cov}} = 2/3$, $d = r_{\text{ej}}$), but these two set of predictions should be considered extremely uncertain.

of times that the photons cross the shell (1 if the XRS is within the shell; 2 if the XRS is outside the shell), and for the inclination of the photon direction with respect to the normal to the shell (note that g can be quite larger than 2 if the line of sight to the XRS is almost tangential to the ejecta shell). Maccarone et al (2010) suggest that the weakness of the XRS in RZ 2109 during the *Chandra* 2010 observation might be explained by a large increase in the effective N_{H} in front of the XRS. We used the web version of W3PIMMS (<http://heasarc.nasa.gov/Tools/w3pimms.html>) to estimate that $N_{\text{H}} \gtrsim 3 \times 10^{22} \text{ cm}^{-2}$ is necessary to explain the *Chandra* 2010 observations. This is marginally consistent with our scenario: if we set $g = 6$, $Z = 0.50$, $m_{\text{ej}} = 2.2 \times 10^{-3} M_{\odot}$, we can obtain such a high N_{H} for $r_{\text{ej}} \lesssim 3 \times 10^{16} \text{ cm}$. In turn, this implies that the nova eruption occurred in 2000–2004 (for $1 \lesssim v_{\text{ej},3} \lesssim 1.5$), which might be consistent with the timing of the Z07 observations (2004–2005). However, the available parameter space is very small: a slight change in the choice of g , Z and m_{ej} can reduce the upper limit on r_{ej} , moving the nova occurrence to an epoch *after* the first Z07 observation. Therefore, we deem quite unlikely that the weakening of the XRS is (entirely) due to the additional absorption from the nova shell; however, if this is the case, the XRS should re-brighten within a few years.

5.3 Probability

We estimate the probability of having a nova shell with properties suitable to explain the RZ 2109 observations within a distance \tilde{d} from the XRS as

$$p(< \tilde{d}) = \Gamma_E \gamma_{\text{GC}} (N_{\text{GC}} \langle m_{\text{GC}} \rangle) \left(\frac{4\pi}{3} \tilde{d}^3 \right) \frac{n_{*,c}}{N_{\text{GC}}} \tilde{f} t_{\text{nova}} \sim \\ \sim 5 \times 10^{-9} \gamma_{\text{GC}} \left(\frac{\langle m_{\text{GC}} \rangle}{0.5 M_{\odot}} \right) \left(\frac{\tilde{d}}{0.1 \text{ pc}} \right)^3 \frac{n_{*,c}}{10^5 \text{ pc}^{-3}} \frac{\tilde{f}}{0.01} \frac{r_{\text{ej}}}{0.01 \text{ pc}} v_{\text{ej},3}^{-1} t_{\text{nova}} \quad (2)$$

where Γ_E and γ_{GC} were introduced in Sec. 2, N_{GC} is the number of stars in a GC, $\langle m_{\text{GC}} \rangle$ is the average stellar mass in a GC, $n_{*,c}$ is the number density of stars at the centre of a GC (10^4 – 10^6 pc^{-3} ; see e.g. Pryor & Meylan 1993), \tilde{f} is the fraction of novae whose ejecta can produce the observed line emission (a highly uncertain quantity; since relatively massive ejecta are needed, we use 0.01 as a reference), and $t_{\text{nova}} \sim 10 \text{ yr} [r_{\text{ej}} / (0.01 \text{ pc})] v_{\text{ej},3}^{-1}$ acts as the visibility timescale for the [OIII] line emission.

Such a probability is of the same order of magnitude as that predicted in other scenarios such as the disruption of a WD by an IMBH (Clausen & Eracleous 2011 quote a disruption rate of $\sim 10^{-8} \text{ yr}^{-1} \text{ GC}^{-1}$ from Sigurdsson & Rees 1997), and it must be noted that the large uncertainty about several parameters in the above formula might lead to a substantial increase of $p(< \tilde{d})$.

We note that, if the XRS is outside the nova shell, a further factor $\Omega/4\pi$ accounting for the possible beaming of the XRS radiation should be introduced into eq. (2): therefore, an observational confirmation of this scenario might disfavour the models of the XRS (e.g. King 2011) that assume a beamed emission⁹.

⁹ Beamed XRS models face problems even when the XRS is within the shell: the emission from gas outside the beam is likely negligible, so that the fluxes of *Cloudy* models assuming $f_{\text{cov}} = 2/3$ (appropriate for this geometry) should be multiplied

6 SUMMARY AND CONCLUSIONS

We used the photoionization code *Cloudy* to check whether the peculiar emission spectra from XRS-hosting GCs (especially RZ 2109) can be explained as the result of the photoionization of a nova shell by the radiation emitted by the XRS. We found that this is definitely possible, but requires that the nova ejecta are relatively massive ($\gtrsim 0.5 \times 10^{-3} M_{\odot}$), and that the XRS-nova distance is quite small ($\lesssim 0.1 \text{ pc}$).

The combination of these two requirements is quite unlikely; on the other hand, it can explain observations in a straightforward manner (although the line profile needs further investigation). While not entirely satisfactory, this compares well with the two other proposed scenarios for RZ 2109: (i) the disruption of a WD by an IMBH (an event as unlikely as the one we discuss) explains the line profile and the absence of H lines (I10, Clausen & Eracleous 2011), but appears to be unable to produce the high [OIII] luminosity (Porter 2010, S11); (ii) the ionization of material ejected from the XRS itself, while not suffering from the “unlikely coincidence” problem, does not explain either the absence of H emission lines, nor some properties of the line profile (asymmetry in the flat component, origin of the gaussian component).

Finally, we predict the future evolution of the line emission in the XRS+nova scenario, by looking at both optical and UV lines. We find that in most cases the nova shell tends to move towards a higher ionization state, so that the line flux should move from moderate-ionization lines such as [OIII] $\lambda 5007\text{\AA}$ to high-ionization lines (e.g. the OVI lines in the 1032–1038 \AA wavelength range). Such predictions might provide a crucial test for discriminating among the various hypotheses described above.

ACKNOWLEDGMENTS

We thank the anonymous referee for a careful reading of the manuscript, and for several very valuable suggestions (e.g. about UV lines), and thank A. Wolter, L. Zampieri, A. Bressan, D. Fiacconi, S. Hachinger, R. Porter, and T. Maccarone for useful discussions and comments. This research has made use of NASA’s Astrophysics Data System Bibliographic Services, and of tools provided by the High Energy Astrophysics Science Archive Research Center (HEASARC; which is provided by NASA’s Goddard Space Flight Center).

REFERENCES

- Allende Prieto C., Lambert D.L., Asplund M., 2001, *ApJ*, 556, L63
- Allende Prieto C., Lambert D.L., Asplund M., 2002, *ApJ*, 573, L137
- Brassington N.J., et al., 2010, *ApJ*, 725, 1805
- Chochol D., Grygar J., Pribulla T., Komzik R., Hric L., Elkin V., 1997, *A&A*, 318, 908
- Clausen D., Eracleous M., 2011, *ApJ*, 726, 34

by a factor of $\leq (\Omega/4\pi)/(2/3)$: if $\Omega/4\pi \lesssim 0.1$, no viable model of this kind would survive.

- Della Valle M., Rosino L., Bianchini A., Livio M., 1994, *A&A*, 287, 403
- Gehrz R.D., Truran J.W., Williams R.E., Starrfield S., 1998, *PASP*, 110, 3
- Ferland G.J., Shields G.A., 1978, *ApJ*, 226, 172
- Ferland G.J., Korista K.T., Verner D.A., Ferguson J.W., Kingdon J.B., Verner E.M., 1998, *PASP*, 110, 761
- Grevesse N., Sauval A.J., 1998, *Space Science Review*, 85, 161
- Heinke C.O., 2011, to appear in the proceedings of the conference “Binary Star Evolution: Mass Loss, Accretion and Mergers” (eds. V. Kalogera and M. van der Sluys, AIP Conf. Ser.), Mykonos, Greece, June 22-25, 2010, (arxiv.org/1101.5356)
- Holweger H., 2001, Joint SOHO/ACE workshop “Solar and Galactic Composition” (Bern, Switzerland, March 6–9 2001), edited by R.F. Wimmer-Schweingruber, AIPC proceedings, vol. 598, p. 23
- Henze M., et al., 2009, *A&A*, 500, 769
- Henze M., et al., 2010, *A&A*, 523, 89
- Iijima T., Naito H., 2011, *A&A*, 526, A73
- Irwin J.A., Brink T.G., Bregman J.N., Roberts T.P., 2010, *ApJ*, 712, L1 [I10]
- Kalogera V., Henninger M., Ivanova N., King A.R., 2004, *ApJ*, 603, L41
- King A., 2011, *ApJ*, 732, L28
- Maccarone T.J., Kundu A., Zepf S.E., Rhode K.L., 2007, *Nature*, 445, 183 [M07]
- Maccarone T.J., Kundu A., Zepf S.E., Rhode K.L., 2010, *MNRAS*, 409, L84
- Maccarone T.J., Kundu A., Zepf S.E., Rhode K.L., 2011, *MNRAS*, 410, 1655
- Maccarone T.J., Warner B., 2011, *MNRAS*, 410, L32
- Mannucci F., Della Valle M., Panagia N., Cappellaro E., Cresci G., Maiolino R., Petrosian A., Turatto M., 2005, *A&A*, 433, 807
- Moore K., Bildsten L., 2011, *ApJ*, 728, 81
- Peacock M.B., Maccarone T.J., Knigge C., Kundu A., Waters C.Z., Zepf S.E., Zurek D.R., *MNRAS*, 402, 803
- Pietsch W., et al., 2007, *A&A*, 465, 375
- Porter R.L., 2010, *MNRAS*, 407, L59
- Prialnik D., 1986, *ApJ*, 310, 222
- Pryor C., Meylan G., 1993, in ASP Conference Series 50, Structure and Dynamics of Globular Clusters, eds Djorgovski S.G. & Meylan G. (San Francisco, CA: ASP), 357
- Shafter A.W., Quimby R.M., 2007, *ApJ*, 671, L121
- Shara M.M., Zurek D.R., Williams R.E., Prialnik D., Gilmozzi R., Moffat A.F.J., 1997, *AJ*, 114, 258
- Shara M.M., Zurek D.R., Baltz E.A., Lauer T.R., Silk J., 2004, *ApJ*, 605, L117
- Shara M.M., Yaron O., Prialnik D., Kovetz A., Zurek D., 2010, *ApJ*, 725, 831 [S10]
- Shih I.C., Kundu A., Maccarone T.J., Zepf S.E., Joseph T.D., 2010, *ApJ*, 721, 323
- Sigurdsson S., Phinney E.S., 1995, *ApJS*, 99, 609
- Sigurdsson S., Rees M.J., 1997, *MNRAS*, 284, 318
- Starrfield S., Truran J.W., Sparks W.M., Kutter G.S., 1972, *ApJ*, 176, 169
- Steele M.M., Zepf S.E., Kundu A., Maccarone T.J., Rhode K.L., Salzer J.J., 2011, *ApJ*, in press (arXiv:1107.4051) [S11]
- Yaron O., Prialnik D., Shara M.M., Kovetz A., 2005, *ApJ*, 623, 398 [Y05]
- Zepf S.E., Maccarone T.J., Bergond G., Kundu A., Rhode K.L., Salzer J.J., 2007, *ApJ*, 669, L69 [Z07]
- Zepf S.E., et al., 2008, *ApJ*, 683, L139 [Z08]

APPENDIX A: FULL PREDICTIONS - TABLES

In this appendix, we list the detailed predictions about line fluxes at Earth, and about the properties of the nova ejecta (e.g. the ionization state of C, N, O, and Ne) from the four models described in the text, evolved to five past or future epochs: April 2005, December 2007, March 2009 (chosen to coincide with the times of past optical observations), December 2012, and December 2017.

We report all the emission lines in the UV-optical range ($913\text{\AA} \leq \lambda \leq 10000\text{\AA}$) reaching a flux $\geq 5 \times 10^{-18} \text{ erg s}^{-1} \text{ cm}^{-2}$ in at least one of the five considered epoch, plus Lyman α and H α . For well-separated multiplets we list only the strongest line (for example, in the case of the [OIII] $\lambda\lambda 4959, 5007\text{\AA}$ doublet we only list [OIII] $\lambda 5007\text{\AA}$), whereas close multiplets are listed as a single line (for example the [OII] $\lambda\lambda 3726, 3729\text{\AA}$ doublet is listed as [OII] $\lambda 3727\text{\AA}$). All the fluxes are in units of $10^{-16} \text{ erg s}^{-1} \text{ cm}^{-2}$, and were obtained assuming a distance $D = 16 \text{ Mpc}$. No reddening correction was applied.

All the data columns - except the one referring to the Z08 observation, which is taken as a reference point - report two set of data: the first was obtained assuming that the shell thickness Δd remains constant at the value used for December 2007 (implying that the density n scales as r_{ej}^{-2} ; assumption a), whereas the second was obtained assuming that Δd increases linearly with time (i.e. that $\Delta d/r_{\text{ej}}$ remains constant at the value estimated for December 2007; in such case the density n scales as r_{ej}^{-3} ; assumption b). The two cases are generally separated by a “/”, but in the case of ionization states it was necessary to use two separate lines.

Table A1. Evolution of emission line fluxes and other physical properties for model A.

Line	April 2005	December 2007	March 2009	December 2012	December 2017
Model A - Spectral lines					
NIII λ 991	0.020/0.014	0.043	0.063/0.074	0.129/0.094	0.077/0.026
OVI λ 1032–1038	0/0	0.005	0.020/0.035	0.232/0.446	0.654/0.900
Lyman α λ 1216	0.168/0.182	0.103	0.081/0.072	0.045/0.033	0.029/0.018
OV] λ 1218	0/0	0.004	0.011/0.016	0.076/0.131	0.170/0.178
NV λ 1239, 1243	0.005/0.002	0.055	0.131/0.189	0.667/0.878	0.977/0.704
OIV] λ 1402	0.004/0.002	0.038	0.090/0.130	0.460/0.548	0.516/0.279
NIV] λ 1486	0.012/0.006	0.081	0.172/0.235	0.714/0.770	0.647/0.267
CIV λ 1549, 1551	0.068/0.004	0.031	0.057/0.071	0.162/0.151	0.119/0.043
OIII] λ 1661, 1666	0.030/0.020	0.092	0.135/0.147	0.168/0.088	0.073/0.025
NIII λ 1750	0.067/0.046	0.196	0.286/0.314	0.383/0.203	0.146/0.037
CIII] λ 1907, 1909	0.026/0.022	0.059	0.078/0.082	0.092/0.049	0.033/0.007
[NeIV] λ 2424	0.007/0.003	0.041	0.085/0.114	0.326/0.348	0.310/0.156
[OII] λ 2471	0.050/0.100	0.014	0.011/0.008	0.004/0.002	0.002/0.001
[NeV] λ 3426	0.003/0.002	0.012	0.023/0.031	0.103/0.153	0.178/0.171
[OII] λ 3727	0.055/0.098	0.012	0.010/0.008	0.005/0.002	0.003/0.001
[NeIII] λ 3869	0.166/0.148	0.232	0.242/0.229	0.139/0.058	0.041/0.010
[OIII] λ 4363	0.030/0.023	0.058	0.071/0.071	0.056/0.025	0.019/0.006
[OIII] λ 5007	2.77/2.24	3.6	3.43/3.14	1.48/0.555	0.385/0.097
[NII] λ 5755	0.023/0.053	0.005	0.004/0.003	0.001/0.001	0.001/0
H α λ 6563	0.014/0.015	0.008	0.006/0.004	0.003/0.002	0.002/0.001
[NII] λ 6583	0.433/0.893	0.055	0.037/0.029	0.012/0.006	0.006/0.001
[OII] λ 7325	0.068/0.140	0.019	0.015/0.012	0.006/0.003	0.003/0.001
Model A - Model parameters and ionization conditions					
$\log n$ [cm^{-3}]	4.87/4.96	4.70	4.63/4.59	4.45/4.33	4.26/4.04
t_{nova} [yr]	10.4	13.1	14.4	18.1	23.1
r_{ej} [10^{16} cm]	4.9	6.2	6.8	8.6	10.9
f_{cov}	0.020	0.030	0.0354	0.533	0.0831
$\log U$ (13.6eV)	-2.98/-3.07	-2.81	-2.74/-2.70	-2.56/-2.44	-2.37/-2.15
C(I \rightarrow VII)	-,11,69,6,13,1,- 0,31,56,5,8,0,-	-,3,55,11,27,4,0	-,2,45,13,33,7,0 -,1,40,13,36,9,1	-,0,17,12,45,23,2 -,0,8,9,44,33,5	-,0,5,6,40,40,9 -,0,1,2,26,50,21
N(I \rightarrow VIII)	0,25,63,7,4,1,-,- 3,48,42,4,2,0,-,-	-,2,70,15,9,4,0,-	-,1,61,20,11,7,1,- -,1,56,22,12,9,1,-	-,0,24,30,15,25,5,0 -,0,11,28,15,35,10,1	-,0,7,21,14,40,16,1 -,0,2,9,9,43,32,5
O(I \rightarrow IX)	0,31,58,9,2,0,0,-,- 3,52,39,6,1,0,-,-,-	-,2,69,23,4,2,0,-,-	-,1,58,31,6,3,1,-,- -,1,53,35,7,4,1,0,-	-,0,19,53,13,10,5,0,- -,0,8,50,18,13,10,1,-	-,0,6,41,20,15,15,2,0 -,2,22,20,17,30,8,0
Ne(I \rightarrow XI)	0,25,69,5,1,0,-,-,-,-,- 2,39,55,3,1,-,-,-,-,-	-,1,79,15,3,0,-,-,-,-,-	-,1,70,23,5,1,-,-,-,-,- -,1,65,27,7,1,0,-,-,-,-	-,0,29,49,19,3,0,-,-,-,- -,0,13,50,30,6,1,0,-,-,-	-,0,10,44,36,9,1,0,0,-,- -,3,26,47,18,4,1,1,0,-

Fluxes are in units of 10^{-16} erg s $^{-1}$ cm $^{-2}$ and assume $D=16$ Mpc (no reddening). Wavelengths are in Å, and in case of multiplets only the strongest component(s) are listed. The ionization states of C,N,O, and Ne are described by listing the percentages of each ionic state with respect to the total (with “0” indicating a percentage between 0.05% and 0.5%, and “-” indicating a percentage below 0.05%). See text for more details

Table A2. Evolution of emission-line fluxes and other physical properties for model B.

Line	April 2005	December 2007	March 2009	December 2012	December 2017
Model B - Spectral lines					
NIII λ 991	0.010/0.002	0.132	0.216/0.220	0.115/0.042	0.038/0.005
OVI λ 1032–1038	0/0	0.032	0.167/0.285	1.06/1.39	1.47/0.961
Lyman α λ 1216	0.523/0.872	0.342	0.245/0.208	0.136/0.094	0.095/0.057
OV] λ 1218	0/0	0.034	0.118/0.173	0.371/0.287	0.234/0.073
NV λ 1239, 1243	0.009/0.002	0.252	0.744/1.01	1.76/1.30	1.09/0.301
OIV] λ 1402	0.007/0.001	0.181	0.495/0.637	0.607/0.268	0.200/0.030
NIV] λ 1486	0.020/0.002	0.341	0.850/1.07	0.982/0.420	0.303/0.040
CIV λ 1549, 1551	0.016/0.002	0.127	0.228/0.250	0.175/0.068	0.045/0.005
OIII] λ 1661, 1666	0.067/0.003	0.306	0.347/0.285	0.077/0.024	0.022/0.002
NIII λ 1750	0.140/0.006	0.655	0.809/0.710	0.221/0.065	0.056/0.004
CH] λ 1907, 1909	0.074/0.053	0.144	0.151/0.128	0.035/0.009	0.006/0
NI] λ 2141	0.205/0.316	0.014	0.009/0.006	0.003/0.001	0/0
CII] λ 2324 – 2329	0.067/0.114	0.007	0.004/0.003	0.001/0	0/0
[NeIV] λ 2424	0.005/0	0.087	0.180/0.206	0.132/0.046	0.028/0.002
[OII] λ 2471	0.546/0.798	0.024	0.011/0.006	0.002/0	0/0
[NeV] λ 3426	0.004/0	0.083	0.204/0.256	0.303/0.168	0.110/0.011
[OII] λ 3727	0.070/0.076	0.004	0.002/0.001	0.001/0	0/0
[NeIII] λ 3869	0.316/0.305	0.358	0.231/0.156	0.017/0.003	0.002/0
[OIII] λ 4363	0.071/0.003	0.206	0.176/0.129	0.024/0.006	0.005/0
[OIII] λ 5007	1.37/0.050	4.84	3.36/2.33	0.368/0.095	0.080/0.005
[NI] λ 5755	0.333/0.500	0.013	0.006/0.004	0.001/0	0/0
[OI] λ 6300	0.336/0.581	0	0/0	0/0	0/0
H α λ 6563	0.027/0.030	0.025	0.017/0.014	0.008/0.005	0.004/0.002
[NI] λ 6583	0.748/0.812	0.027	0.013/0.008	0.004/0.001	0.001/0
[OII] λ 7325	0.726/1.06	0.033	0.015/0.009	0.002/0	0/0
Model B - Model parameters and ionization conditions					
$\log n$ [cm ⁻³]	5.83/6.00	5.50	5.38/5.32	5.10/4.90	4.82/4.48
t_{nova} [yr]	4.7	7.4	8.7	12.4	17.4
r_{ej} [10 ¹⁶ cm]	2.2	3.5	4.1	5.9	8.2
f_{cov}	0.0139	0.030	0.0399	0.0759	0.1429
$\log U$ (13.6eV)	-3.01/-3.18	-2.68	-2.56/-2.50	-2.28/-2.08	-2.00/-1.66
C(I→VII)	1,60,33,2,3,0,-	-2,41,14,36,6,0	0,1,24,14,47,14,1	-0,4,7,44,39,6	-0,1,2,26,52,19
	2,74,24,0,0,-,-		-0,18,13,49,19,1	-0,1,3,32,50,14	-,-,0,0,9,46,46
N(I→VIII)	20,63,14,2,1,0,-,-	-1,65,19,9,5,0,-	-1,43,29,14,13,1,-	-0,7,23,18,40,11,1	-0,2,8,11,46,29,3
	33,66,1,0,-,-,-,-		-0,32,31,15,18,2,0	-0,3,11,14,48,23,2	-,-,0,1,3,30,50,15
O(I→IX)	32,52,13,2,0,-,-,-,-	-1,62,28,6,2,1,-,-	-0,36,44,11,6,2,0,-	-0,4,34,25,18,17,1,-	-,-,1,12,18,22,40,8,0
	43,56,0,-,-,-,-,-,-		-0,25,49,14,8,4,0,-	-,-,1,16,22,23,33,5,0	-,-,0,2,6,11,52,26,2
Ne(I→XI)	5,39,52,3,0,-,-,-,-,-	-1,60,28,10,2,0,-,-,-,-	-0,33,38,23,6,1,0,-,-,-	-,-,3,20,42,27,6,2,1,0,-	-,-,0,5,24,36,19,10,6,0,-
	8,47,45,0,-,-,-,-,-,-		-0,22,39,29,9,1,0,-,-,-	-,-,1,8,32,36,14,6,3,0,-	-,-,-,0,4,15,20,24,35,1,0

See the caption of Table A1 for the definition of symbols and units.

Table A3. Evolution of emission-line fluxes and other physical properties for model C.

Line	April 2005	December 2007	March 2009	December 2012	December 2017
Model C - Spectral lines					
CIII λ 977	0.349/0.308	0.284	0.247/0.223	0.175/0.125	0.116/0.069
NIII λ 991	1.140/1.130	0.878	0.751/0.656	0.529/0.348	0.359/0.180
OVI λ 1032–1038	2.360/1.180	2.090	1.920/2.270	1.380/2.090	0.880/1.620
Lyman α λ 1216	0.332/0.448	0.212	0.178/0.161	0.121/0.088	0.078/0.044
OV] λ 1218	0.890/0.505	0.717	0.631/0.722	0.413/0.550	0.240/0.331
NV λ 1239, 1243	4.930/3.100	4.240	3.810/4.160	2.670/3.070	1.690/1.790
OIV] λ 1402	3.850/2.590	3.160	2.730/2.740	1.760/1.570	1.030/0.736
NIV] λ 1486	6.590/4.400	5.400	4.640/4.640	2.960/2.510	1.690/1.060
CIV λ 1549, 1551	1.940/1.300	1.570	1.340/1.340	0.842/0.694	0.467/0.282
OIII] λ 1661, 1666	1.150/1.580	0.733	0.605/0.473	0.439/0.230	0.321/0.115
NIII λ 1750	3.210/4.040	2.200	1.820/1.450	1.280/0.659	0.889/0.295
CIII] λ 1907, 1909	1.230/1.470	0.867	0.722/0.581	0.497/0.261	0.329/0.114
[OIII] λ 2321	0.113/0.184	0.059	0.047/0.034	0.032/0.015	0.022/0.006
[NeIV] λ 2424	1.520/1.000	1.460	1.340/1.340	0.982/0.855	0.637/0.447
[NeV] λ 3426	0.865/0.546	0.713	0.631/0.705	0.423/0.536	0.248/0.322
[NeII] λ 3869	0.964/1.620	0.528	0.425/0.315	0.301/0.130	0.218/0.055
[OIII] λ 4363	0.485/0.789	0.254	0.200/0.149	0.136/0.063	0.095/0.028
[OIII] λ 5007	9.350/16.90	4.630	3.720/2.680	2.730/1.150	2.050/0.498
H α λ 6563	0.023/0.033	0.014	0.012/0.010	0.008/0.006	0.005/0.003
[NII] λ 6583	0.032/0.054	0.036	0.038/0.032	0.048/0.026	0.056/0.017
Model C - Model parameters and ionization conditions					
$\log n$ [cm^{-3}]	5.19/5.29	5.00	4.92/4.88	4.73/4.60	4.52/4.28
t_{nova} [yr]	9.2	11.9	13.2	16.9	21.9
r_{ej} [10^{16} cm]	4.3	5.6	6.2	8.0	10.3
f_{cov}	2/3	2/3	2/3	2/3	2/3
$\log U(13.6\text{eV})$	-2.58/-2.68	-2.58	-2.57/-2.53	-2.58/-2.45	-2.57/-2.33
C(I \rightarrow VII)	-1,34,17,37,11,1 -,1,50,14,28,6,0	-1,26,17,41,14,1	-1,24,17,42,15,2 -,1,20,16,44,18,2	-2,25,15,42,15,2 -,1,13,12,45,25,4	-2,26,14,41,15,2 -,1,10,8,41,33,8
N(I \rightarrow VIII)	-0,30,34,12,20,4,0 -,0,49,27,10,12,2,0	-0,21,35,13,25,5,0	-0,20,34,14,26,6,0 -,0,15,33,14,29,8,1	-1,20,32,14,27,6,1 -,0,10,26,14,36,13,1	-1,23,29,14,26,7,1 -,0,8,17,12,39,21,3
O(I \rightarrow IX)	-0,21,51,12,9,6,1,- -,0,39,42,9,6,3,0,-	-0,12,53,15,12,8,1,-	-0,11,51,15,12,8,1,- -,0,8,49,17,13,10,2,0	-0,12,48,16,13,9,1,- -,0,6,39,19,15,17,4,0	-1,14,45,16,13,10,2,0 -,0,5,28,18,16,24,8,1
Ne(I \rightarrow XI)	-0,29,48,19,4,1,0,-,-,- -,0,49,37,12,2,0,0,-,-,-	-0,20,52,23,5,1,0,-,-,-	-0,18,52,24,5,1,0,0,-,- -,0,14,51,28,6,1,0,0,-,-	-0,20,49,24,5,1,0,0,-,- 0,0,10,44,35,9,2,1,0,-,-	0,0,23,47,23,5,1,0,0,-,- -,0,8,36,40,12,3,1,1,0,-

See the caption of Table A1 for the definition of symbols and units.

Table A4. Evolution of emission-line fluxes and other physical properties for model D.

Line	April 2005	December 2007	March 2009	December 2012 ^(a)	December 2017 ^(a)
Model D - Spectral lines					
CIII λ 977	0/0	0.061	0.063/0.039	0.003/0	0.002/0
NIII λ 991	0/0	0.213	0.208/0.138	0.009/0	0.005/0
OVI λ 1032–1038	0/0	0.371	1.41/1.83	0.714/0.093	0.309/0
Lyman α λ 1216	0.391/0.411	0.403	0.191/0.145	0.040/0.015	0.023/0
OV] λ 1218	0/0	0.149	0.492/0.599	0.050/0.003	0.021/0
NV λ 1239, 1243	0/0	0.746	2.01/2.27	0.155/0.013	0.050/0
OIV] λ 1402	0/0	0.493	1.11/1.09	0.028/0.001	0.014/0
NIV] λ 1486	0/0	0.784	1.72/1.65	0.018/0.001	0.009/0
CIV λ 1549, 1551	0/0	0.216	0.456/0.391	0.006/0.001	0.003/0
[NeIV] λ 1602	0/0	0.086	0.161/0.142	0.006/0.001	0.003/0
OIII] λ 1661, 1666	0/0	0.296	0.198/0.088	0.003/0	0.002/0
NIII λ 1750	0.001/0	0.697	0.496/0.251	0.004/0	0.003/0
CIII] λ 1907, 1909	0.008/0.004	0.242	0.173/0.086	0.001/0	0.001/0
NII] λ 2141	0.118/0.092	0.005	0.002/0.001	0/0	0/0
CII] λ 2324 – 2329	0.062/0.063	0.005	0.002/0.001	0/0	0/0
[NeIV] λ 2424	0/0	0.137	0.341/0.348	0.023/0.003	0.013/0
[OII] λ 2471	0.283/0.200	0.007	0.002/0.001	0/0	0/0
MgII λ 2796, 2803	0.065/0.031	0.004	0.001/0	0/0	0/0
[NeV] λ 3426	0/0	0.127	0.394/0.473	0.059/0.005	0.026/0
[NeI] λ 3467	0.056/0.084	0	0/0	0/0	0/0
[NeIII] λ 3869	0.079/0.062	0.355	0.151/0.051	0.001/0	0.001/0
[OIII] λ 4363	0/0	0.173	0.088/0.031	0.001/0	0/0
[OIII] λ 5007	0.007/0.002	4.30	1.73/0.480	0.005/0	0.003/0
[NII] λ 5755	0.185/0.168	0.005	0.001/0.001	0/0	0/0
[OI] λ 6300	0.348/.454	0	0/0	0/0	0/0
H α λ 6563	0.022/0.030	0.031	0.014/0.010	0.002/0.001	0.001/0
[NII] λ 6583	0.244/0.159	0.013	0.003/0.001	0/0	0/0
[OII] λ 7325	0.375/0.264	0.010	0.003/0.001	0/0	0/0
Model D - Model parameters and ionization conditions					
$\log n$ [cm ⁻³]	6.20/6.55	5.50	5.30/5.20	4.46/4.15	4.11/3.63
t_{nova} [yr]	1.5	4.2	5.5	9.2	14.2
r_{ej} [10 ¹⁶ cm]	0.7	2.0	2.6	4.3 ^(a)	6.7 ^(a)
f_{cov}	0.02	0.10	0.160	2/3 ^(a)	2/3 ^(a)
$\log U$ (13.6eV)	-3.28/-3.63	-2.58	-2.38/-2.28	-1.76/-1.44	-1.76/-1.28
C(I→VII)	41,57,2,-,-,-,-,-	-,2,65,8,20,5,0	-,0,20,12,40,22,4	-,-,0,0,4,30,66	-,-,0,0,5,31,63
	59,40,1,-,-,-,-,-		-,0,7,10,42,33,8	-,-,,-,-,1,15,85	-,-,,-,-,-,3,97
N(I→VIII)	74,26,0,-,-,-,-,-	-,1,68,15,7,8,2,0	-,0,21,27,12,28,10,1	-,-,0,0,0,9,42,48	-,-,0,0,0,9,41,48
	80,20,-,-,-,-,-,-		-,-,7,25,12,36,17,2	-,-,,-,-,-,2,23,75	-,-,,-,-,-,0,5,95
O(I→IX)	70,30,0,-,-,-,-,-,-	-,1,64,23,6,4,3,0,-	-,0,18,40,16,11,12,3,0	-,-,0,1,1,2,21,49,26	-,-,0,1,1,2,20,49,26
	76,24,-,-,-,-,-,-,-		-,-,4,39,19,13,18,6,0	-,-,,-,-,0,0,6,38,56	-,-,,-,-,-,0,10,90
Ne(I→XI)	61,30,10,-,-,-,-,-,-,-	-,1,67,21,10,2,0,0,-,-,-	-,0,20,40,31,8,1,1,0,-,-	-,-,0,3,15,21,14,11,27,9,1	-,-,1,3,15,20,13,11,28,9,1
	71,23,6,-,-,-,-,-,-,-,-		-,-,6,38,40,12,3,1,1,0,-	-,-,0,0,2,5,5,6,39,35,6	-,-,,-,-,-,-,0,8,46,46

See the caption of Table A1 for the definition of symbols and units.

Note: ^(a): In this model, the 2012 and 2017 epochs have $r_{\text{ej}} > d$ (the distance between the XRS and the nova), i.e. the XRS becomes engulfed in the expanding nova shell. Then, for these epochs we assume $f_{\text{cov}} = 2/3$, and use r_{ej} as the distance from the XRS to the shell; this is quite inaccurate, but the emission lines remain very weak also for more detailed calculations.